2014

Experimental Analysis of R134a and R1234ze(E) Flow Boiling Inside a Roll Bond Evaporator

Giulia Righetti
University of Padova, Department of Management and Engineering, I-36100 Vicenza, Italy., giulia.righetti@studenti.unipd.it

Claudio Zilio
University of Padova, Department of Management and Engineering, I-36100 Vicenza, Italy., claudio.zilio@unipd.it

Giovanni A. Longo
University of Padova, Department of Management and Engineering, I-36100 Vicenza, Italy., tony@gest.unipd.it

Experimental Analysis of R134a and R1234ze(E) Flow Boiling Inside a Roll Bond Evaporator

Giulia RIGHETTI[1], Claudio ZILIO[1], Giovanni A. LONGO[1]

[1]University of Padova, Department of Management and Engineering,

I-36100 Vicenza, Italy.

giulia.righetti@studenti.unipd.it

ABSTRACT

This paper presents an experimental study of R134a and R1234ze(E) inside an off the shelf roll bond evaporator, commonly used for small size domestic refrigerators. The evaporator was mounted inside a climate dark chamber where ambient temperature and humidity were maintained stable during the tests. To control the inlet conditions (evaporation temperature, inlet quality, refrigerant mass flow rate) it was used a water cooled miniature scale vapor cycle system with R134a and R1234ze(E) as working fluids. By means of an IR-thermo-camera and thanks to 16 thermocouples collocated on the back of the evaporator, the whole roll bond temperature field was investigated under different working conditions. During the experimental tests the refrigerant mass flow rate was varied by regulating the compressor speed, while ambient temperature and evaporation temperature were kept as constant. From the IR pictures it was possible to delineate the super heating region and to point out the areas of the evaporator in which heat transfer is less efficient depending on the fluid and on the working conditions. The data acquired from the vapor cycle system (i.e. condensation and evaporation pressure, evaporator inlet quality, vapour superheating, refrigerant mass flow rate) coupled with the IR thermo-camera images allowed to evaluate the behavior and the efficiency of the roll bond. Since the data were collected maintaining the same operating conditions in term of ambient temperature and humidity, heat flow rate and evaporation temperature, it was possible to highlight differences among the two refrigerants in terms of mass flux. Furthermore, on the basis of the IR images and of the thermocouples measurements, an average heat transfer coefficient was defined and determined both on the air and the refrigerant side. The average heat transfer coefficients of the two refrigerants are compared and outlined in the paper.

1. INTRODUCTION

The global annual production of domestic refrigerators and freezers is more than 80 million units (Björk (2010)) and a great number of that use roll bond type evaporators. Despite that, only few scientific studies focus on this component and on its own behavior, while a greater number of works examine the whole refrigerator system.

Da Silva et al. (1999) experimentally measured the heat transfer rate as a function of the evaporator positioning within the food compartment. Björk and Palm (2008) investigated the flow boiling heat transfer in a evaporator varying the mass flux, the heat flux and the vapor quality. Porkhial et al. (2004) collected some data points to validate a numerical model during the start-up of the system.

In the last years in many cooling applications variable refrigerant flow rate modulation has been proposed to enhance the efficiency and this technology is going to be applied also in the domestic refrigerator field. In the open literature is possible to find some works that analyze the transient period during ON-OFF control, for example Hermes et al. (2008), Berger et al. (2012) and Porkhial et al. (2004). But there are no studies that analyze the problem under the variable flow rate approach point of view. For this reason it has been chosen to examine the evaporator behavior focusing on several steady state conditions at different mass flow rate, to simulate a variable speed system.

Recently, European Commission has approved a new release of the F-Gas regulation, stating that refrigerants with GWP> 150 cannot be anymore used in new domestic refrigerators starting January 2015. So it is mandatory to find a suitable low GWP, low flammability, substitute for R134a, which has been the most used refrigerant in this specific application for years.

Hydrocarbons, such as R600a (Isobutane) and R290 (Propane), have been already used in small domestic refrigerators and drink-coolers especially in Europe and in Asia. In the literature is possible to find some performance comparisons between R134a and R600a, or hydrocarbon mixtures, (Mahmood et al (2013), Rasti et al. (2013), Mohanraj (2013)) and it is possible to appreciate a performance enhancement of the system correlated to a reduction of the optimum amount of refrigerant charge, but hydrocarbons are classified as flammable. The HFOs, especially the R1234yf and R1234ze(E) are other suitable candidates to replace the high GWP fluids.

In this paper it is presented a performance comparison in terms of heat transfer coefficient among R134a and R1234ze(E) in order to highlight quality and weakness of the new refrigerant.

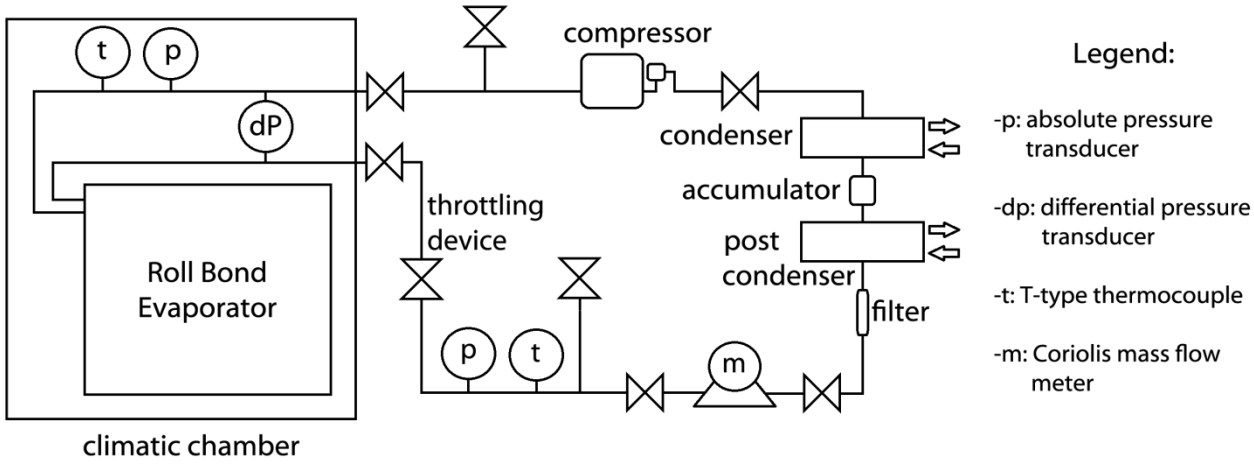

Figure 1: Schematic view of the experimental rig

2. EXPERIMENTAL SET UP

To simulate the behavior of a domestic refrigerator, the experimental facility consists of four main components: a roll bond evaporator, which is the subject of the analysis, a compressor, a condenser and a throttling device.
Figure 1 shows a schematic of the test rig, including the locations of the measurement devices and some of the additional components essential to run the facility.
The compressor is a 1.9 cm^3 rotary model made by Aspen. The compressor is driven by a DC brushless motor with variable speed control.
The condenser is split in two water cooled tube-in-tube heat exchangers. Each of them is fed by a thermostatic bath so it is possible to control the condensing and the subcooling temperatures independently. Therefore the desired specific enthalpy and vapor quality can be set at the inlet of the roll bond evaporator.
A liquid accumulator is placed among the two heat exchangers to ensure the necessary amount of refrigerant during high load tests.
Once out of the condenser, the fluid finds a filter then it passes through the throttling device (a Swagelok metering valve).
By suitably tuning the compressor rotation speed and the throttling valve stem position it is possible to set the refrigerant mass flow rate at the evaporation pressure.
The evaporator is put inside a climate test chamber at 3°C to reproduce the refrigerate cavity of the fridge.
The chamber is a Weiss WK111-180 model with a internal volume of 750x580x450 mm, able to maintain the air temperature deviation within ±1 K (spatial distribution) and ±0.3 K (time).
To monitor air temperature during experimental tests, two T-type thermocouples were positioned inside the chamber: one about 3 cm above the floor and the other one about 3 cm below the ceiling.
Air velocity inside the chamber is the minimum value to avoid excessive air stratification (within 1 K) and it is comparable to air velocity of real domestic refrigerators. It has also been mounted a desiccant rotor (Munters MG 50) with a rated airflow of 50 m^3/h to limit the humidity inside the chamber. Thanks to this device the chamber air dew temperature was kept below -5°C in all the tests reported in this paper.
The roll bond evaporator studied in this work is an off the shelf component, normally used for small domestic refrigerators. A scheme of the geometry and the main dimensions are reported in Figure 2 and Table 1 respectively.
The evaporator back face has been covered with a thick layer of flexible insulation so that just the front face is able to exchange heat, than the whole system has been hung up on the internal climate chamber wall.
To evaluate the temperature field during experimental tests 16 T-type (Copper-Constantan) thermocouples (uncertainty (k= 2) within ±0.1 K) have been attached on the aluminum plate, among the roll bond rear face and the insulation panel. Their spatial distribution is represented in Figure 2.
In addition, an infrared camera (Agema, Thermovision 550, temperature uncertainty (k= 2) within ±0.1 K) has been positioned in front of the evaporator.

Table 1: Characteristics of the roll bond evaporator.

Ratio external/internal heat transfer area	1.69
Plate lenght L (m)	0.42
Plate widht W (m)	0.52
Plate thickness (m)	0.0008
Tube section perimeter (m)	0.347
Tube section area (m^2)	$1.26\ 10^{-5}$

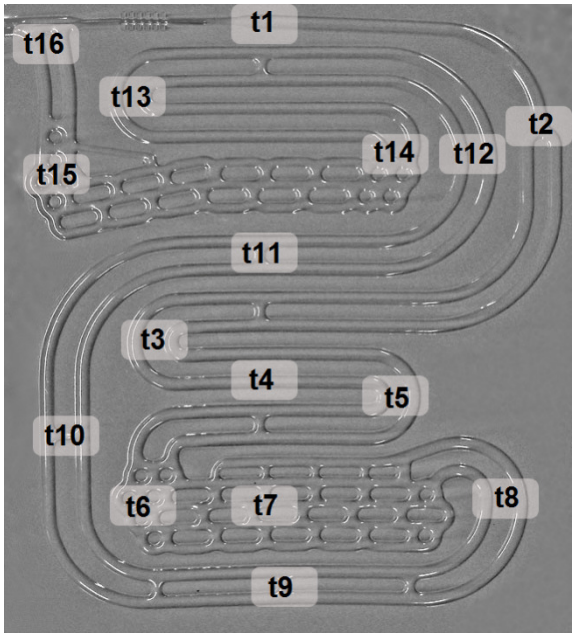

Figure 2: Schematic view of the roll bond evaporator and of the thermocouples positioning.

The measurement set-up was competed as follow:
- a Coriolis mass flow meter (uncertainty (k = 2) within ±0.1 % of the reading) has been used to measure the refrigerant mass flow rate;
- three strain gauge absolute pressure transducers were positioned at the outlet of the evaporator (uncertainty (k = 2) within ± 0.075% f.s.), at the inlet of the throttling device (uncertainty (k= 2) within ± 0.075% f.s.) and at the compressor discharge (uncertainty (k = 2) within ± 0.5% of the upper range limit respectively). In addiction two T-type thermocouples (uncertainty (k = 2) within ±0.1 K) were placed inside adiabatic mixing chambers, one just before the throttling valve and one at the evaporator outlet. For the measured temperatures and pressures it is possible to evaluate specific enthalpy and refrigerant quality at the evaporator inlet and the specific enthalpy at the evaporator outlet.

3. DATA REDUCTION

Once steady state conditions in temperature, pressure and refrigerant mass flow are reached, all the data collected are scanned and recorded by a data logger for a set time after which an average value is computed for each parameter.
From the average values of the measurements recorded during the steady state conditions, it is possible to compute the following characteristic parameters:

1) Heat flow rate Q

$$Q = \dot{m}\,(h_{out} - h_{in}) \tag{1}$$

where ṁ is the refrigerant mass flow measured by the Coriolis mass flow meter and h_{in} and h_{out} are the specific enthalpies at the inlet and outlet of the roll bond evaporator respectively.

2) Specific heat flux q

defined as the ratio between the heat flow rate Q and the tube surface that is the product of the tube wetted perimeter P and the length of the tube.

$$q = \frac{Q}{P\,l} \tag{2}$$

2) Mean overall heat transfer coefficient U

$$U = \frac{Q}{A\,(t_a - t_r)} \tag{3}$$

where A= L x W is the surface area of the whole front face of the evaporator; t_a is the mean value between two T-type thermocouples respectively installed close to the floor and to the ceiling of the climate chamber and t_r is the refrigerant saturation temperature evaluated thanks to Refprop 9.1 (2013)

3) Mean air heat transfer coefficient α_a

$$\alpha_a = \frac{Q}{A\,(t_a - t_w)} \tag{4}$$

where t_w is the mean value of 16 thermocouples positioned on the rear face of the roll bond evaporator.
Also in this case the area A is the frontal surface of the evaporator.

4) mean refrigerant heat transfer coefficient α_r

that derives from the overall heat transfer coefficient, assuming no fouling resistances and neglecting the wall resistance:

$$\alpha_r = \frac{1}{\left(\frac{1}{U} - \frac{1}{\alpha_a}\right)\left(\frac{A}{A_t}\right)} \tag{5}$$

where A_t is the plate surface occupied by the tube in which the refrigerant flows.

4. ANALYSIS OF THE RESULTS

Two different sets of experimental tests were carried out on the same roll bond evaporator, at the same chamber air temperature (3°C) and humidity. The first one has been carried out using R134a and the second one with R1234ze(E),
To highlight differences among the two fluids, the mean refrigerant heat transfer coefficient α_r has been compared at the same specific heat flux.
For each fluid two different evaporation temperatures has been investigated: -15°C and -20°C, while condensing temperature has been fixed around 40°C and subcooling temperature was between 20 and 30 °C, depending on the refrigerant mass flow rate.
Each series of data points has been run varying the refrigerant mass flow, ranging from the minimum value achievable by the compressor up to the maximum where no more superheating was displayed at the evaporator outlet.

Table 2: Operating conditions during experimental tests.

Experimental data set	t cond	t sub	x in	G
	(°C)	(°C)	(-)	(kg/(m^{2}s))
R134a (t_{evap}=-15°C)	40—42	21—33	0.26—0.32	11—49
R134a (t_{evap}=-20°C)	40—43	21—34	0.27—0.35	11—60
R1234ze(E) (t_{evap}=-15°C)	41—42	22—25	0.27—0.28	10—50
R1234ze(E) (t_{evap}=-20°C)	40—41	21—24	0.28—0.30	10—56

Table 2 summarizes the operating conditions during experimental tests: evaporation temperature t_{evap}, condensation temperature t_{cond}, subcooling temperature t_{sub}, inlet refrigerant vapor quality x_{in} and refrigerant mass flux G.
A detailed error analysis following the method suggested by Kline and McClintock (1954) is reported in Table 3.

Table 3: Mean uncertainty values evaluated by Kline and McClintock (1954) method.

Uncertainty	
Specific enthalpy	±1 % (*)
Evaporator cooling capacity	±2.9 %
Overall heat transfer coefficient	±7.6 %
Air heat transfer coefficient	±2.0 %
Refrigerant heat transfer coefficient	±20.0 %
(*) (Estimated from the measured values of temperature and/or pressure using RefProp v9.1(2013)	

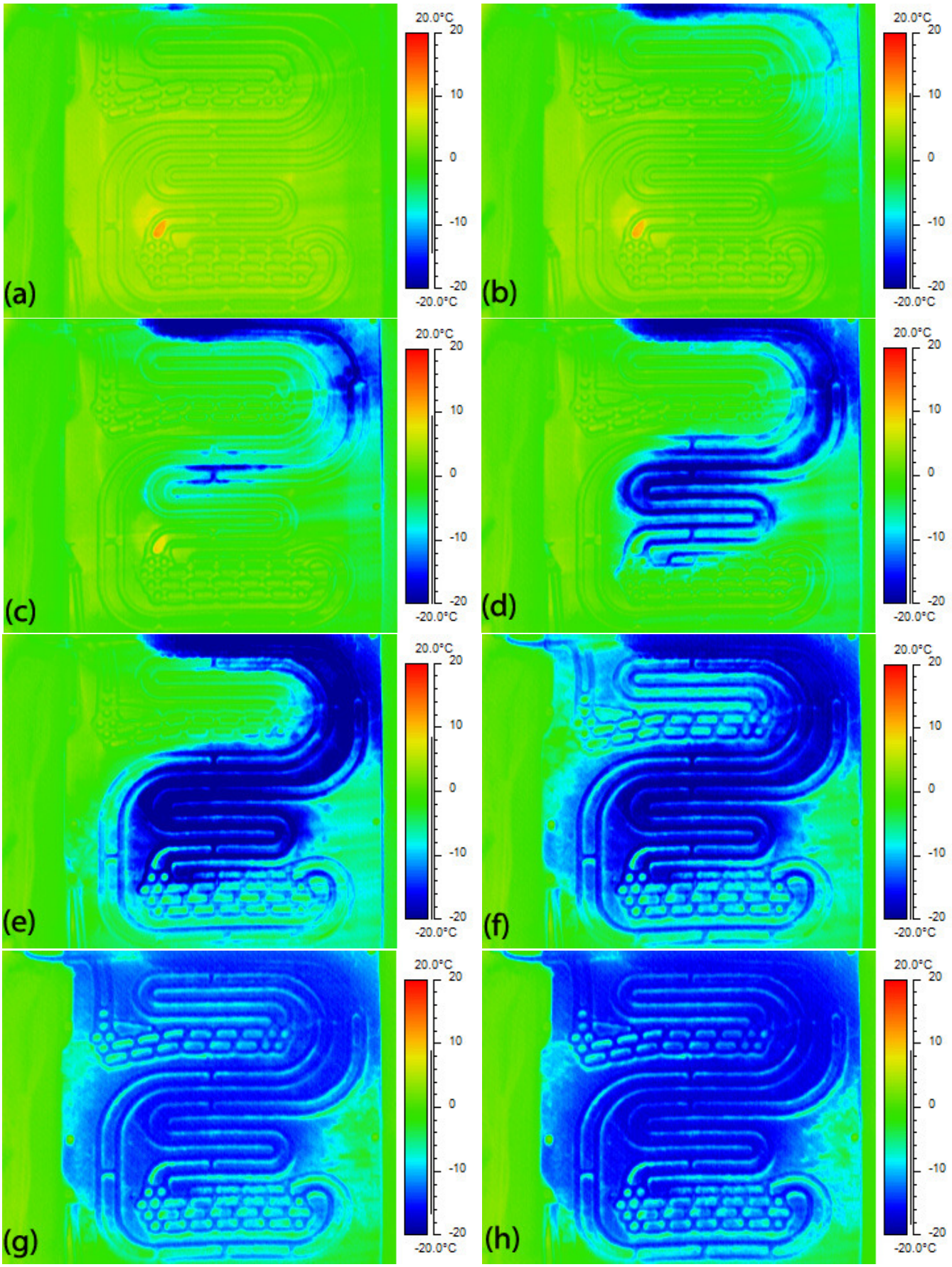

Figure 3: Roll bond images collected by the thermal camera. Data with R134a at t_{evap}=-15°C. Refrigerant mass flow rate: (a) ṁ=0.51 kg/h; (b) ṁ=0.76 kg/h; (c) ṁ=0.99 kg/h; (d) ṁ=1.27 kg/h; (e) ṁ=1.55 kg/h; (f) ṁ=1.76 kg/h; (g) ṁ=2.07 kg/h; (h) ṁ=2.24 kg/h.

As mentioned, a infrared (IR) camera was utilized to observe the temperature distribution on the front face of the roll bond evaporator.

Images from 3(a) to 3(h) reported in Figure 3 have been taken at steady state conditions at different mass flow rates. They show a good agreement in temperatures with the corresponding wall thermocouples so they can be taken as a valid way to analyze this problem.

The coldest areas are painted in dark blue, while the hottest are in red. The green color corresponds to approximately 0°C and shows the superheating surfaces.

In Figure 3 are reported eight pictures taken during experimental tests with R134a at t_{evap}=-15°C. Space limit restrictions preclude to include pictures of other tests conditions, but there are no differences between the two fluids image series. A saturation temperature of -20°C carries to a shift in IR picture colors toward colder temperatures but the global behavior remains the same.

At a first glance it is possible to observe that increasing the mass flow rate and thus the heat capacity, the superheating area decreases. In addiction it can be noticed that the two channels are not fed in the same way by the liquid (Images 3(c) and 3(d)). The little bridges among them are useful to equalize the liquid mass flow rate (Image 3(c)).

Furthermore, especially in Figure 3(c) one can notice a thermal bridge between the liquid line in the first bend and the superheated vapor going toward the outlet. The more the mass flow is limited, the more this phenomena is marked, in fact when the whole plate has approximately the same wall temperature the effect of "thermal bridging" tends to vanish.

Understanding the fluid-dynamics helps to properly design the heat exchanger in appliances working with variable speed compressors. For instance, Figures 3(a) to 3(e) indicate that particular care should be taken for the circuitry lay-out for part load functioning, whereas at full load operation (Figures 3(g) and 3(h)) this is not an issue.

Figure 4 shows the refrigerant heat capacity versus the refrigerant flow rate. Heat capacity can be fairly considered as linear function of the refrigerant mass flow rate.

There is no appreciable difference between the two fluids and the two saturation temperatures. So R1234ze(E) can be surely considered an environmentally friendly substitute for R134a, provided that the compressor displacement is adjusted to deliver the proper refrigerant mass flow rate.

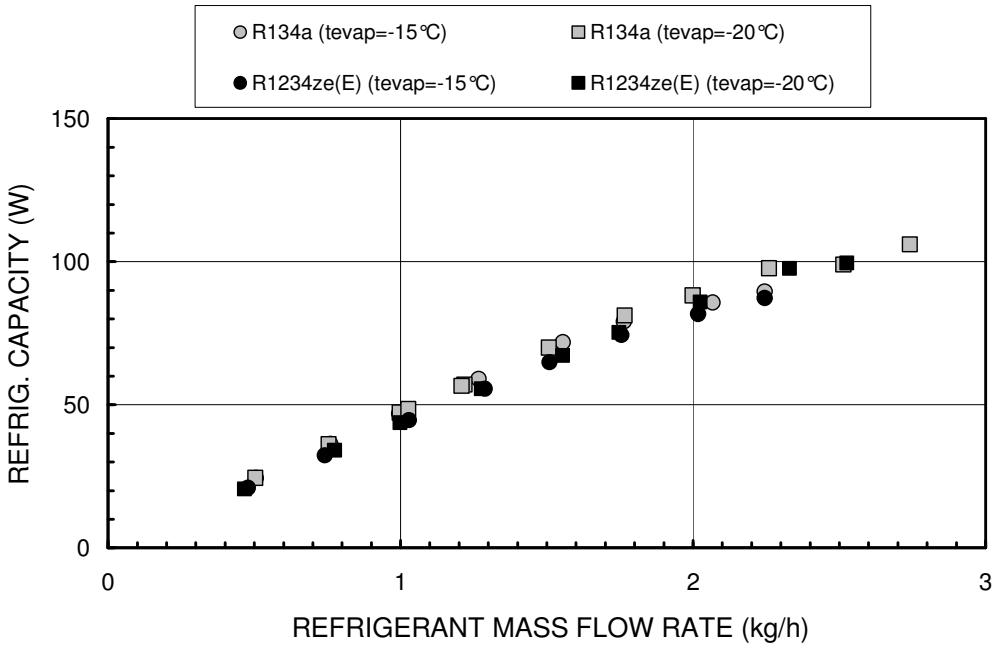

Figure 4: Refrigerant capacity vs. refrigerant mass flow rate

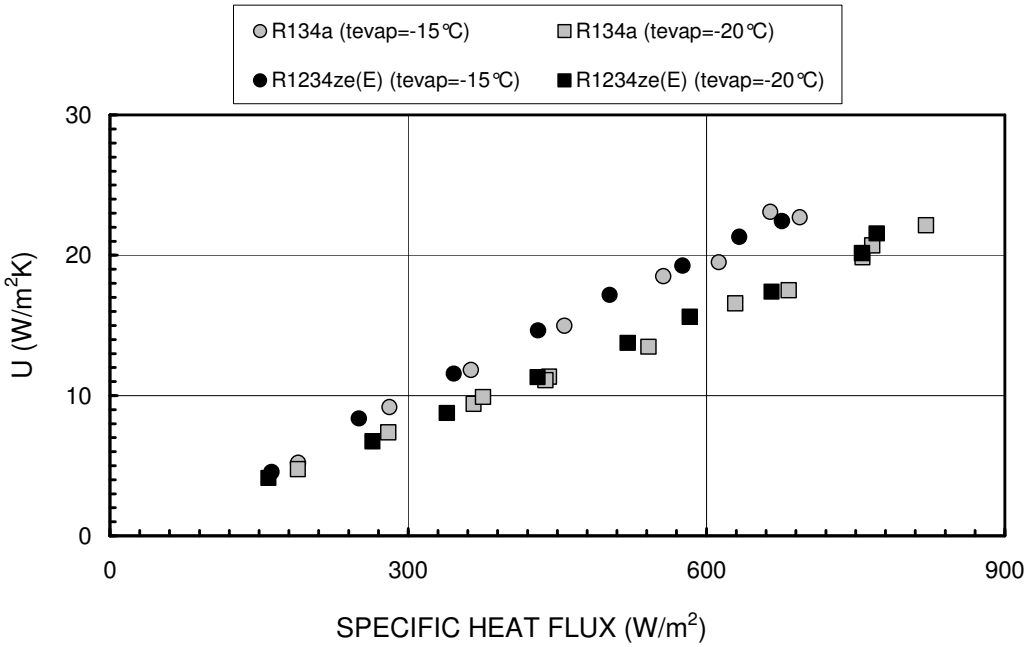

Figure 5: Overall heat transfer coefficient vs. specific heat flux

For each evaporating temperature the mass flow rate upper limit is fixed by the roll bond geometry. In fact at the maximum mass flow rate (conditions as in Figure 3(g) and 3(f)) the vapour superheating at the evaporator outlet is less than 1K and almost all the heat transfer area is interested by two-phase heat transfer.

The air side heat transfer coefficient obtained from experimental measures is a constant value, and it does not depend on saturation temperature, type of fluid and mass flow. The mean α_a value of all the data points is 22.0 W/(m^{2}K) with absolute mean standard deviation of 2.1 W/(m^{2}K) .

This coefficient has been evaluated on the roll bond front face only, because the rear face has been insulated and treated as adiabatic.

In Figure 5 is plotted the overall heat transfer coefficient as a function of the refrigerant mass flow rate. One can notice that it shows a linear dependence on the mass flow rate and so on the specific heat flux. The sets of data collected at t_{evap}=-20°C present a overall heat transfer slightly lower (-13%) than those collected at t_{evap}=-15°C.

Figure 6 reports the refrigerant heat transfer coefficient as a function of the specific heat flux.

Also in this graph the heat transfer coefficient data collected at t_{evap}=-20°C are lower (-32%) than those of the data at t_{evap}=-15°C. The difference between the two series is more evident at higher heat fluxes.

Al low mass flow rates, the refrigerant heat transfer coefficients are very low because all of them are referred to the whole plate surface. Thus it is hard to appreciate differences among the series in this part of the graph.

According to the recorded data, the mass flux ranged between 10 and 60 kg (m^2/s), with heat flux between 160 W/m^2 and 820 W/m^2. These values are extremely low and fall outside the validity range of all the common correlations for boiling heat transfer inside tubes. Furthermore, the circuitry lay-out is characterized by horizontal tube stretches, vertical segments, bends and the particular "embossed" arrangement in the two "accumulators" (see Figure 2). Finally, the tube cross section looks like a flattened tube, with external fins. No dedicated heat transfer coefficient models have been proposed so far in the literature for this very particular tube arrangement. A general comment can be inferred, the Reynolds number of the liquid phase, evaluated at the average vapour quality (i.e. x=0.67, fairly constant in all the tests) was always below 150. As a matter of fact, in the very well known classical Chen correlation (1966) for flow boiling inside tubes, the suppression factor for the pool boiling contribution approaches 1 at low liquid Reynolds numbers, while the convective boiling contribution has poor effect, given the rather low liquid Reynolds number. Accordingly, the refrigerant heat transfer coefficients at the maximum mass flux have been compared against the correlation valid for pool boiling proposed by Cooper (1984).

$$\alpha_{tp} = 55\, p^{*^{(0.12-0.2\, log_{10}R_p)}} (-log_{10}p^*)^{-0.55}\, q^{0.67} M^{-0.5} \tag{6}$$

where p* = p/p_{cr} is the reduced pressure, R_p (μm) the roughness as defined in German standard DIN 4762/1, q is the heat flux and M the molecular weight of the fluid.

The Cooper correlation (1984), reported in Figure 6 as a solid line for R1234ze(E) and dotted line for R134a, reproduces this data points with an absolute mean standard deviation of 7% in the case of R134a and of 3% with R1234ze(E).

Only two points for each series can be evaluate against a correlation, namely conditions as in Figure 3(g) and 3(h). For lower refrigerant mass flow rates it was not possible to precisely evaluate the actual two-phase area, so the heat transfer coefficients are defined conventionally as per equation (5) considering the whole heat transfer area and, as mentioned before, only conditions (g) and (h) of Figure 3 fulfill this working condition.

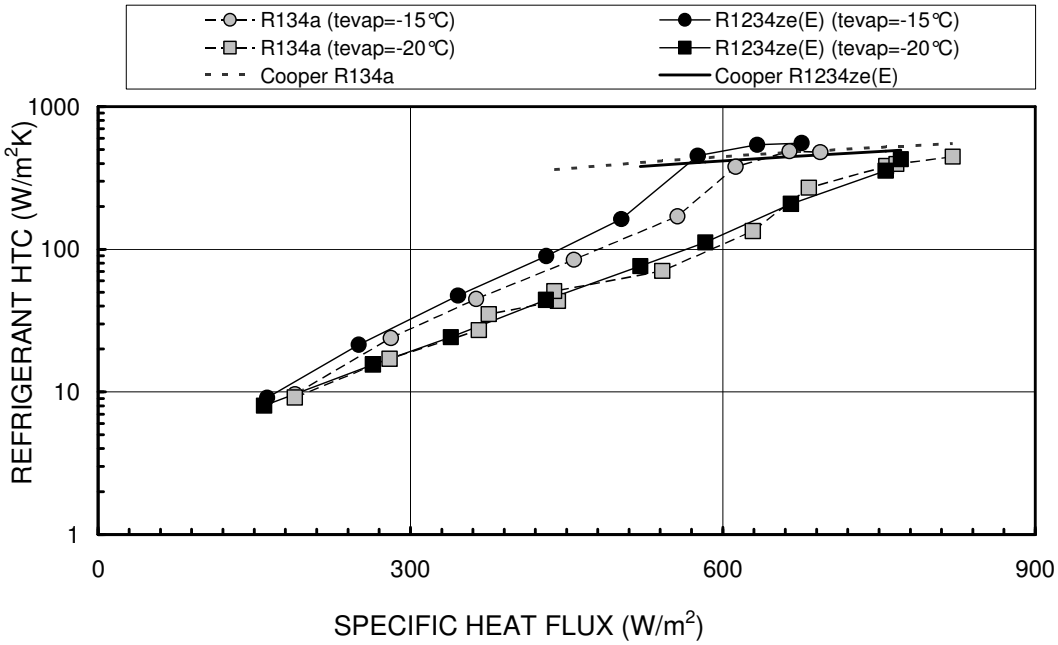

Figure 6: Average heat transfer coefficient on the refrigerant side vs. specific heat flux

CONCLUSIONS

This paper analyzes the performance of an off-the-shelf roll bond type evaporator during steady state conditions. The problem has been investigated under the point of view of a variable flow rate approach, focusing on numerous steady state conditions at different mass flow rates.

Given the European Regulation pressure to the phase out of HFC refrigerants in domestic appliances, it is mandatory to find a low GWP substitute for R134a, in terms of energy efficiency and safety, so two refrigerants have been compared (R134a and R1234ze(E)).

For each fluid two different saturation temperatures (-20°C and -15°C) have been taken into account. Thank to a thermal camera and to 16 T-type thermocouples, the wall temperature distribution has been measured and the main issues related to different refrigerant mass flow rates have been highlighted, with emphasis on the thermal bridge between the superheating area and the two phase region.

In addiction the refrigerant capacity, the overall heat transfer coefficient and the air side and refrigerant side heat transfer coefficient have been evaluated and compared.

The test campaign demonstrated that:

- The refrigerant capacity is a linear function of the mass flow rate, while the air side coefficient is almost constant for all the collected data points (average value 22.0 W/m^{2}K).
- The overall heat transfer coefficient is slightly lower for t_{evap}= -20°C and shows a linear dependence on specific heat flux.

-The refrigerant heat transfer coefficient is higher for t_{evap}= -15°C and increases with the specific heat flux.

For the data points where almost all the internal heat transfer area is interested by two-phase flow, the experimental heat transfer coefficient was compared against the Cooper correlation (1984) showing good agreement (average mean standard deviation 5%).

The study points out that the two refrigerants have the same heat transfer performances in the investigated roll bond heat exchanger, so R1234ze(E) can be surely considered an environmentally friendly substitute for R134a from the point of view of the evaporator design.

NOMENCLATURE

A	one face surface area	(m^2)
c_p	specific heat capacity	(J/(kgK))
d	hydraulic diameter = 4 s /P	(m)
f.s.	full scale	(–)
h	specific enthalpy	(J/kg)
k	thermal conductivity	(W/(mK))
l	tube length	(m)
L	roll bond length	(m)
ṁ	refrigerant mass flow	(kg/s)
M	molar mass	(kg/kmol)
p	pressure	(bar)
p*	reduced pressure $p^* = \frac{p}{p_{cr}}$	(–)
P	tube wetted perimeter	(m)
q	specific heat flux	(W/m^2)
q_{ONB}	onset of nucleate boiling heat flux	(W/m^2)
Q	heat flow rate	(W)
Re	Reynolds number	(–)
Re_L	Liquid Reynolds number $Re_L = \frac{G(1-x_m)d}{\mu_L}$	(–)
R_p	roughness	(µm)
s	cross sectional area	(m^2)
t	temperature	(°C)
U	overall heat transfer coefficient	($W/(m^2K)$)
W	roll bond width	(m)
x	refrigerant quality	(–)

Greek symbols

α	heat transfer coefficient	($W/(m^2K)$)
µ	dynamic viscosity	(Pa s)
ρ	density	(kg/m^3)
σ	surface tension	(N/m)

Subscript

a	air
cb	convective boiling
cr	critic
evap	evaporation
G	gas
in	inlet
IR	infra red
L	liquid
m	mean
max	maximum
nb	nucleate boiling
out	outlet
r	refrigerant
s	subcooling
t	tube
tp	two phase
w	wall

REFERENCES

Berger, E., Heimel, M., Almbauer, R., Lang W., 2012, 1D Heat Exchanger Simulation to Capture the Cycling Transients of Domestic Refrigeration Appliances Working with R600a, *International Refrigeration and Air Conditioning Conference at Purdue*, July 16-19.

Björk, E., Palm, B., 2006, Performance of a domestic refrigerator under influence of varied expansion device capacity, refrigerant charge and ambient temperature, *Int J Refrig,* vol. 29: p. 789 – 798.

Björk, E., Palm, B., 2008, Flow boiling heat transfer at low flux conditions in a domestic refrigerator evaporator, *Int J Refrig* vol. 31: p. 1021 – 1032.

Björk, E., Palm, B., Nordenberg, J., 2010, A thermographic study of the on-off behavior of an all-refrigerator, *Appl Therm Eng,* vol. 30: p. 1974 – 1984.

Chen, J.C., 1966, Correlation for Boiling Heat Transfer to Saturated Fluids in Convective Flow, *I&C Process Design and Development*, vol.5, no. 3: p. 322- 329.

Cooper, M.G, 1984, Heat flows rates in saturated pool boiling – a wide ranging examination using reduced properties, *Advanced in Heat Transfer*, Academic Press, Orlando, Florida, pp: 157–239.

Da Silva, L.W., Melo, C., Pereira R.H., 1999, Heat Transfer Characteristics Of Plate-Type Evaporators, *20th International Congress of Refrigeration*, IIR/IIF, Sydney.

Hermes, C.J.L., Melo, C., Negraõ, C.O.R., 2008, A numerical simulation model for plate-type, roll-bond evaporators, *Int J Refrig,* vol. 31: p. 335 – 347.

Kline, S.J., McClintock, F.A., 1954, Describing uncertainties in single-sample experiments, *Mech. Eng.*, vol. 75: p. 3-8.

Lemmon, E.W., Huber, M.L, McLinden, M.O., 2013 NIST Standard Reference Database23: Reference fluid Thermodynamic and Transport Properties- REFPROP, Version 9.1, NIST, Gaithersburgh.MD.

Mohanraj M., 2013, Energy performance assessment of R430A as a possible alternative refrigerant to R134a in domestic refrigerators, *Energy for Sustainable Development*, vol. 17, p: 471–476.

Porkhial, S., Khastoo, B., Saffar-Avval M., 2004, Transient response of dry expansion evaporator in household refrigerators, *Appl Therm Eng,* vol. 24: p. 1465 – 1480.

ACKNOWLEDGEMENT

This research project was partially funded by:

CariVerona Foundation, Verona, Italy, Ricerca Scientifica e Tecnologica, Sviluppo di innovativi processi a ridotto impatto ambientale per la conservazione e distribuzione a bassa temperatura delle derrate alimentari a salvaguardia della salute, 2013-2014.